Investigation of Accelerated Monte Carlo Techniques for PET Simulation and 3-D PET Scatter Correction

C.H. Holdsworth, *Student Member, IEEE*, C.S. Levin*, *Member, IEEE*, T.H. Farquhar, *Student Member, IEEE*, M. Dahlbom, *Member, IEEE*, E.J. Hoffman, *Fellow, IEEE*
UCLA School of Medicine and UCSD School of Medicine*

Abstract

We have been developing Monte Carlo Techniques for calculating primary and scatter photon distributions in PET. Our first goal has been to accelerate the Monte Carlo Code for fast PET simulation. Our second goal has been to use the simulation to analyze scatter effects in PET and explore the potential for eventual use in scatter correction of clinical 3-D PET studies. We have reduced the execution time to about 30 minutes or ~1 million coincidences per minute. This allows us rapid feedback for the close examination of the accuracy of the simulation. The simulated sinogram matches the original normalized sinogram to within 5% for a low noise level of 2.5% achieved by summing over many planes. We present techniques used to improve computational efficiency of Monte Carlo simulations and photon transport. We use the method to analyze how scatter from within the body, outside the FOV, and from scanner shielding as well as the chosen energy threshold affect 3-D PET sinograms.

I. Introduction

The accuracy of Monte Carlo simulations is primarily limited by the accuracy of the input data and the approximations that are utilized in the particular system model. The input data for our simulation is (1) the initial reconstructed PET image, which is our activity distribution map, and (2) a segmented attenuation image derived from a short transmission scan taken before or after injection of the isotope, which is our physical attenuation map. The scanner system model is based on the Siemens/CTI ECAT EXACT HR+ 962 PET system.

The primary positive result of this work is the significant improvement in the execution time of the simulation. The reduced execution time has allowed us to start a program of investigating PET using the Monte Carlo approach without having to wait a full day for each result. In addition, the reduced execution time makes the Monte Carlo Scatter Correction for 3-D PET feasible for use in the clinic.

To obtain a 5-fold increase in sensitivity, PET scanners can be operated in 3-D mode by removing the inter-ring septa. This increases data acquisition rates by allowing coincidences along lines of response between non-adjacent detector rings. The cost of the greater sensitivity is an increase in the fraction of random and scatter events and an upper limit on the injected dose due to difficulties with dead time.

The long scintillation decay time of BGO crystals (300 ns) has led to a coincidence timing window of 12ns and dead times greater than a μsec, so random events and dead time are a significant problem for 3-D PET studies. As a result, 3-D PET thorax imaging using BGO detectors tends to be inferior to 2-D PET studies. When LSO (40 ns decay time) PET scanners become available, a shorter coincidence timing window (~4-6 ns) and lower dead_time (~200-400 ns) should tip the scales in favor of 3-D PET thorax imaging.

For 2-D PET thorax imaging, one or both photons have been scattered in 10-20% of all coincidences. This fraction increases to 40%-60% when the septa are removed for 3-D PET thorax imaging. This severely degrades image contrast and compromises quantitative accuracy. An accurate scatter correction must be employed before 3-D PET can become widely accepted[1].

Some scatter corrections are independent of source distribution and attenuating media. These methods result in large errors when employed on raw data with a 50% scatter fraction. Activity distribution and attenuation media dependent scatter correction methods show more promise for accuracy[1,2,3]. In this paper we intend to present a fast implementation of a Monte Carlo simulation of 3-D pet that could be used for scatter correction[1,2].

II. Materials and Methods

A. Simulation

To evaluate the accuracy of our simulation, we used emission and transmission data with a very large number of events to minimize noise. The Monte Carlo PET Simulation Code was written in C-language. All simulations were run on a 300MHz dual processor Sun UltraSparc2 Workstation. Although the simulation has 2-D capabilities, all analysis in this paper was achieved using the simulation in 3-D mode.

The simulation requires an activity distribution, which is obtained from the emission image volume. We currently use the system's simulation-based scatter correction[3] during reconstruction of the image to provide an initial activity distribution as close to the true distribution as possible.

The simulation also requires a physical attenuation map that is obtained from the reconstructed transmission image. Once the attenuation map is reconstructed, the image can be smoothed and segmented to provide a low noise attenuation map[4]. Because the attenuating properties of soft tissue and

0-7803-5696-9/00/$10.00 (c) 2000 IEEE

bone are similar in the energy range of our simulation, all voxels corresponding to soft tissue and bone are assigned the same value during segmentation. Voxels corresponding to lung are smoothed to reduce noise while preserving distinct attenuation values. A very low threshold value is then used on the attenuation map to set all air voxels to zero. As a final step, any 'air gaps', such as armpits or the space between the subject and patient bed, are assigned an attenuation value very close to zero. This is done so photons that have escaped all attenuating media can be identified when they land in a voxel with a μ-value of zero. These photons are immediately translated to the detector gantry.

Once the required data is read into memory, the relative number of annihilations in each voxel is determined by the activity distribution. No annihilations are allowed to take place in air. Annihilation photons are transported through the medium using the attenuation map and random numbers to determine interactions. If a Compton events occurs, the new direction of the scatter photon is determined using the Klein-Nishina formula and the resulting energy is calculated. Once a photon escapes the body, it is transported to the detector gantry where it can be detected. If both photons from an annihilation are detected, either a scatter or primary coincidence is recorded, depending on the photons' energies. After all annihilations in every voxel of the activity distribution have been simulated, the program outputs the scatter and primary sinograms to a file.

B. Phantom

We obtained emission and transmission input for our simulation from a 3-D PET acquisition of a thorax phantom with two 10.3cm diameter cold lung inserts of density .2 gm/ml. The major axis of the phantom is 36.1cm, and the minor axis is 23.1cm. A heart phantom with a cold center chamber surrounded by two hot concentric chambers is in the center of the thorax phantom. The heart has a 10.7cm diameter central chamber with 1.2cm and 1.3cm thick annular chambers about the central chamber. An image of the phantom is shown in figure 1.

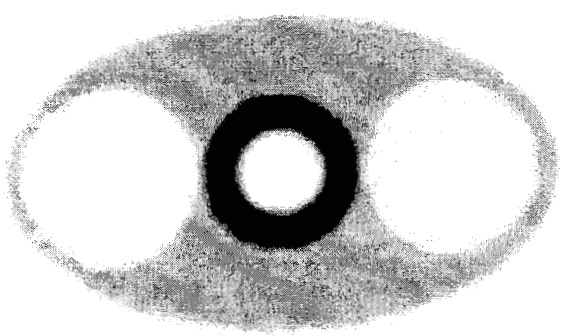

Figure 1. 3-D Pet emission image of phantom used for simulation.

C. Approximations of Simulation

In PET studies, photons will often interact at depth in the detector crystals or pass through undetected. To increase the number of detected events in our simulation, any photon hitting a detector's surface is detected at that point. Errors due to ignoring depth of interaction or scatter in the crystals will have small effects on resolution but very little effect on the scatter distribution. The spatial distribution of penetrating events is also nearly equivalent to that of detected events. Thus, we use this assumption for greater efficiency with insignificant loss in accuracy.

Positron range and the non-colinearity of annihilation photons will degrade resolution slightly; however, they have negligible effect on the scatter distribution. In addition, the resolution of the emission image from which we obtain our activity distribution has already been degraded by these and other effects. For these reasons, we do not incorporate these effects into our system model.

Only Compton scatter events are considered in our simulation. Compton scatter contributes to >99% of all annihilation photon interactions above 317keV[5], which is the simulation's energy threshold. So this approximation can be made without a significant loss in accuracy.

Random coincidence events and dead time are not part of the system model. These effects increase noise but have little effect on the scatter distribution.

All of these approximations are made in the interest of saving computation time. They can be restored or added, but total run time will be affected.

D. Techniques for Reducing Execution Time

The primary difficulty with Monte Carlo Simulation is the long execution time. Therefore, most of our effort was spent optimizing the code for fast execution. In the following paragraphs, we present techniques employed to speed up Monte Carlo PET simulations.

Unnecessary output operations are inefficient and can significantly contribute to total run time. We have eliminated all output from our original code[1], except for writing the final simulation sinograms and an update print statement after the completion of each simulated plane of activity.

Since each annihilation event is independent, the program can be run on different processors in parallel. By using both processors of an UltraSparc2, computation time is halved. We also tested different optimization compilers and now use the most efficient one.

By only allowing photons within an initial axial acceptance angle limit, we avoid simulating annihilations that are unlikely to result in coincidences[1]. By using an acceptance angle limit of 40°, we acquire 4.6 times the number of coincidences for the same execution time with negligible effect on the resulting sinograms.

Due to spaces between detectors both axially and transaxially in the CTI HR+, only about 81% of the gantry surface is actually detector surface, the remaining 19% is air gaps. The photons that enter these air gaps account for 34%

of our coincidences. By assuming no space between the detectors, all photons hitting the gantry are detected, and we avoid losing these events. This increases the total number of detected events by a factor of 1.5 for the same computation time.

Since we are only recording coincidence events, it is not necessary to simulate the second photon of an annihilation pair if the first photon drops below the energy threshold or is undetected. Because only ~20% of the photons that are simulated are actually detected (incorporating the previous techniques), this shortens the runtime by an additional factor of 1.6.

Computers usually calculate functions such as sine, cosine, etc. using a Taylor Series expansion, which involves many operations. By storing values for these functions in arrays with high precision, the calculation can replaced by a single memory access. In addition, the attenuation coefficients for tissue at different energies are also stored in arrays. By implementing this in the code, we achieved an additional factor of 1.5 reduction in execution time.

To further reduce run time, we stored large blocks of random numbers in arrays rather than using a random number generator. In addition, the natural log of random numbers (necessary for photon transport) was stored in a separate array. One risk of this technique is that the relatively short cycle of numbers might affect simulation results. When we compared simulations with and without tabulated random numbers, no significant difference could be observed. By tabulating these random numbers, computation time is reduced by an additional factor of 1.5. We are still investigating efficient random number generators that would not add significantly to execution time.

In our original code[1,2], transporting photons took up more than two thirds of the total computation time. We were using a boundary finding method that would step through the attenuation medium to determine the distance to the next boundary. It would then use this distance to determine the probability of interaction and then transport the photon to the appropriate location (either boundary edge or point of interaction).

To speed up the code, we developed an interpolation-subtraction method of photon transport that calculates a random attenuation distance product, $(\mu \cdot d)_{ran}$. It then steps the photon through the medium subtracting the μ-value of each voxel times the step size from $(\mu \cdot d)_{ran}$. If $(\mu \cdot d)_{ran}$ reaches zero before the photon exits the body, then an interaction occurs at that point. As each photon jumps from one voxel to the next, the μ-values of both voxels are averaged to minimize error. By using this method, total execution time was cut in half.

For even greater efficiency, we are currently using the Delta Scattering Photon Transport algorithm[6]. This method transports each photon a random distance assuming the maximum attenuation coefficient for the entire volume. The probability of interaction at the new location is determined by the quotient of that voxel's μ-value divided by the largest μ-value. The photon will continue to be transported in this manner until it escapes the body or falls below the energy threshold. Using this method reduces the run time by an additional factor of 2.9 over the original method[1]. Minor discrepancies are observed near the water lung boundaries, but these effects are extremely small and worth the reduction of computation time.

A significant improvement in the efficiency of the program was the result of many minor adjustments and algorithmic simplifications incorporated to streamline the code. We tried to make the program as efficient as possible without reducing accuracy.

Our code currently acquires 30million coincidences resulting from 600million annihilations in 30 minutes. This allows us to do many simulations per day. Subtle changes in the code can be made and tested quickly, giving rapid feedback on the accuracy of the simulation. Different effects, such as energy threshold, can also be studied rapidly with small parameter changes so that accurate results can be obtained in 30 minutes. The reduced computation time is also necessary if we want to employ the simulation as a 3-D PET scatter correction in the clinic.

III. Results

A. Accuracy

Because of the short execution time, we were able to look in detail at energy threshold, axial acceptance angle limit, processing for attenuation map and activity distribution, and other variables that might affect the accuracy of the simulation. In this manner we were able to achieve a high level of accuracy while keeping the code as efficient as possible. Figure 2 shows a comparison of profiles for one angle for the simulated totals sinogram (scatter + primary) and the normalized measured sinogram. The difference between these sinograms is <5% for a noise level of 2.5%. The low level of noise was obtained by using a high statistics simulation (150 million counts) and by smoothing both sinograms over 5cm axially.

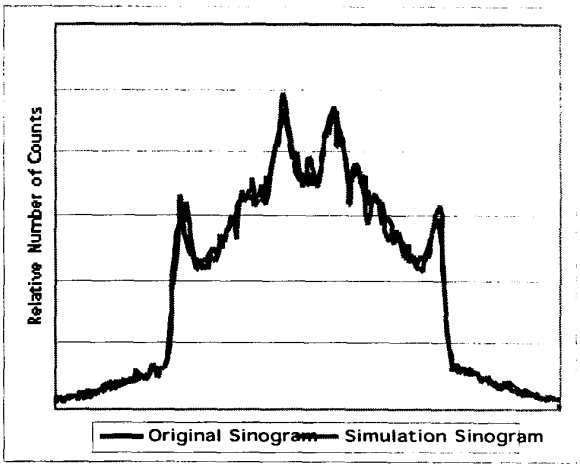

Figure 2. Comparison between the simulated totals and the original measured sinogram data without scatter correction for an AP view through both lungs.

Once we were satisfied with the accuracy, we were able to use the simulation to analyze different effects on the scatter distribution. We were able to look at how energy threshold, scatter from outside the FOV, attenuation by the patient bed, and the lead shielding affect the scatter distribution. We also used the simulation to correct for scatter in phantom images.

B. Effects of Energy Threshold

When we used a 350keV energy threshold for our simulation, the resulting scatter distributions were different than that of the original measured data. Figure 3 shows the effect of different energy thresholds on the simulated total sinograms. Using a lower energy threshold results in a higher scatter fraction and a broader distribution. By repeating the simulation using different energy thresholds, we found that using an effective energy threshold of 317keV gave the most accurate results (used for figure 2).

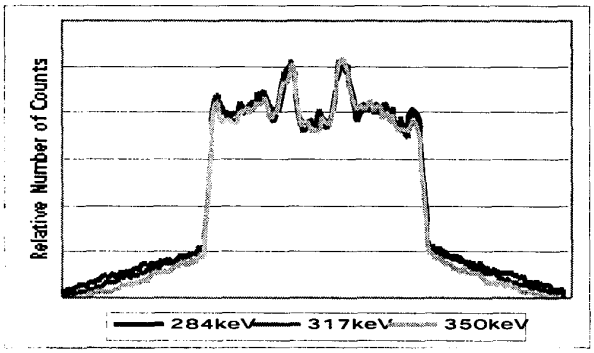

Figure 3. Simulation sinogram profiles of an angle across the narrow axis of the phantom shows the differences in the thorax sinogram for the three energy thresholds. The sinograms were smoothed over 5cm axially to reduce noise.

The reason the 317keV energy threshold is more accurate than the manufacturer suggested 350keV threshold may be due to the ~20% energy resolution of the system. Photons with energies below the nominal energy threshold are being accepted along lines of response that fall outside of the phantom. It would be possible to simulate the ~20% energy resolution, but it is much more computationally efficient to find an effective energy threshold that mimics the behavior of the system.

C. Scatter from Outside the Field of View

It is possible for scatter coincidences to result from annihilations that occur outside the axial FOV. The most obvious effect of out of FOV scatter can be seen primarily in the significant discrepancies just outside the phantom wall. Simulated sinograms with and without FOV scatter are compared in figure 4. Our phantom was only 26cm long in the axial direction, so the full activity distribution could be modeled with less than two bed positions. It is important to determine at what point outside the axial FOV the annihilations no longer make a significant contribution to the scatter distribution for different activity configurations. We want to maintain a high level of accuracy while keeping run time to a minimum.

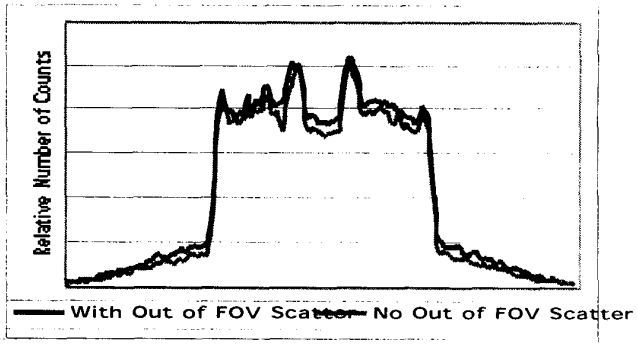

Figure 4. Compares simulation sinogram profiles of an angle across the narrow axis of the phantom with and without scatter from outside the FOV. The sinograms were smoothed over 5cm axially to reduce noise.

D. Effect of Attenuation by the Patient Bed

In an earlier version of our code we ignored attenuation by the patient bed. The simulation sinograms resulting from that program did not match the original sinogram; thus, we incorporated the patient bed into our model. The effect of attenuation through the patient bed is shown in figure 5.

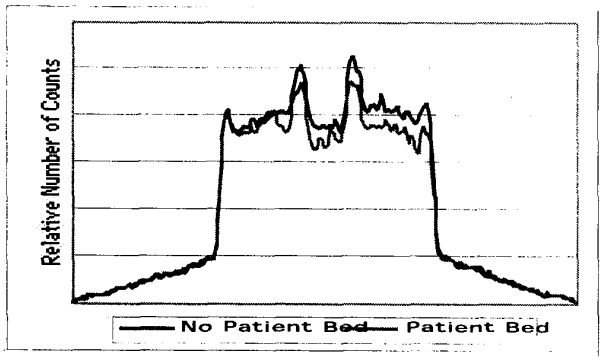

Figure 5. Compares simulation sinogram profiles of an angle across the vertical axis of the phantom with and without the effect of attenuation by the patient bed. Profiles are smoothed over 5cm axially to reduce noise.

Attenuation by the bed causes a significant gradient in the sinogram profile that decreases toward the patient bed. Because noise in clinical transmission scans can result in significant error in the attenuation map of the bed, it is best to acquire a single long transmission image of the patient bed alone. This information can then be used in the input attenuation map for any simulated study.

E. Lead Shielding

We were interested in learning how the lead shields at the ends of the axial field of view affect the scatter distribution, and whether or not they need to be incorporated into our simulation. First, we analyzed the contribution of photon

scatter off lead shields to the scatter distribution. Through simulation, we found that less than 0.5% of all events are due to scatter off of the lead shielding at the edge of the axial FOV, so we ignore this effect in our current program.

We also wanted to see how not having the lead shields to intercept photons might effect the scatter distribution. For a phantom whose active axial length was only 26cm, there was negligible effect on the scatter distribution, so we did not consider the shields in our simulation. We plan to test for this effect again on larger activity distributions.

F. Scatter Correction

This simulation can be used to scatter correct 3-D PET studies. The scatter contribution in the simulated images can be scaled and subtracted from the normalized sinograms of the original study prior to reconstruction.

Figure 6 shows image profiles before and after using the Monte Carlo scatter correction. A significant amount of scatter can be seen in the central heart chamber of the uncorrected image profile. Using the Monte Carlo simulation, we can accurately correct for the contribution due to scatter. The low scatter in the lung region is believed to be due to the low attenuation of the lungs and its correction.

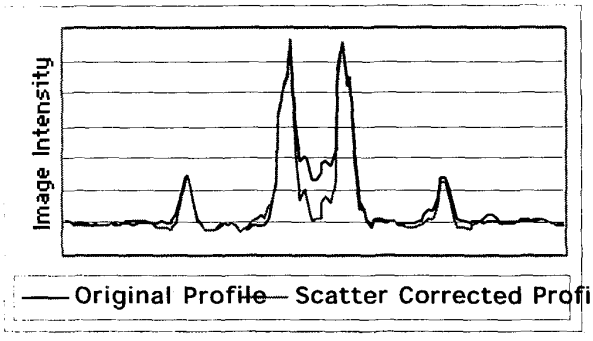

Figure 6. A comparison of profiles taken horizontally through the center of the measured image and Monte Carlo scatter corrected image.

In order to apply the Monte Carlo Scatter Correction to 3-D PET studies in the Clinic, one would first reconstruct the emission image for the activity distribution using the scatter correction method already on the system[2] for a best first estimate of the activity distribution. The run time is significant for 3-D reconstruction using the PROMIS algorithm[7]. The transmission scan would then be processed to obtain the attenuation map (reconstructed in 2-D). After this very brief step, the scatter sinogram can be calculated using the Monte Carlo simulation. After subtracting off the scatter fraction from the original normalized sinogram, the resulting sinogram can be 3-D reconstructed to produce the final image. Thus, the time of the simulation as well as one extra 3-D reconstruction is the greater time cost of employing the Monte Carlo Scatter Correction. As computer efficiency improves this will become less and less of a problem.

Generous smoothing can be employed to the scatter distribution due to its low frequency nature. For this reason, we anticipate that less than 30million simulated events will be required to make an accurate scatter correction. This could drastically reduce the simulation time. In addition, improvements are still being made on the program.

For future work, we plan to compare the accuracy of our Monte Carlo scatter correction with other techniques currently available. We also want to study performance on phantom distributions with varying noise levels and eventually on patient data for clinical 3-D PET thorax studies.

IV Conclusion

Our Accelerated Monte Carlo Simulation of ECAT HR+ 3-D PET scan acquires ~1million events per minute. The simulation is accurate to <5% for a noise level of 2.5%. We have seen that the simulation is an effective tool for analyzing scatter effects in 3-D PET studies. The code is now fast enough that we can look at the effectiveness of employing the simulation as a scatter correction in the clinic. We plan to compare the Monte Carlo Scatter correction to other techniques and continue to work on improving the code.

V. Acknowledgments

The authors would like to thank Yiping Shao and Indrin Chetty for valuable discussions concerning Monte Carlo techniques. This work was funded in part by NCI grant R01-CA56655 and DoE Contract DEF G0387-ER6061.

VI. References

[1] C.S. Levin, Y. Tai, M. Dahlbom, T.H. Farquhar, E.J. Hoffman, "Removal of the effect of compton scattering in 3D whole body PET by Monte Carlo", *1995 Nuclear Science Symposium and Medical Imaging Conference Record*, vol. 2, pp. 1050-54, October 1995

[2] C.S. Levin, M. Dahlbom, and E.J. Hoffman, "A Monte Carlo correction for the effect of Compton scattering in 3-D PET brain imaging," *IEEE Transactions on Nuclear Science*, vol. 42, pp. 1181-85, August 1995

[3] C.C. Watson et al, "Evaluation of simulation-based scatter correction of 3D Cardiac Imaging," *IEEE Transactions on Nuclear Medicine*, vol. 44, pp. 90-97, February 1997

[4] S.R. Meikle, M. Dahlbom, and S. Cherry, "Attenuation correction using count-limited transimission data in Positron Emission Tomography," *Journal of Nuclear Medicine*, vol. 34, pp.143-150, January 1993

[5] H.E. Johns and J.R. Cunningham, The Physics of Radiology, Springfield, Charles C Thomas, 1983, pp. 723-33

[6] E.R. Woodcock et al, "Techniques Used in the GEM Code for Monte Carlo Neutronics Calculation", *Proceeding on the Conference for Applications of Computing Methods to Reactors*, ANL-7050, pp. 557, 1965

[7] P.E. Kinahan and J.G. Rogers, "Analytic 3D image reconstruction using all detected events," *IEEE Transactions on Nuclear Science*, vol. 36, pp. 964-68, 1989